

**TWO-GRID STRATEGY FOR UNSTEADY STATE  
NONLINEAR SCHRÖDINGER EQUATIONS**

Li Wu

Department of Mathematics  
University of Rhode Island  
Kingston, RI 02881-0816, USA  
e-mail: liwu@math.uri.edu

**Abstract:** Two-grid mixed finite element schemes are developed for solving nonlinear Schrödinger equations. The schemes use discretizations based on a mixed finite-element method. The two-grid approach yields iterative procedures for solving the nonlinear discrete equations. The idea is to relegate all of the Newton-like iterations to grids much coarser than the final one, with no loss in order of accuracy. Numerical tests are performed.

**AMS Subject Classification:** 35K57, 65M60

**Key Words:** nonlinear Schrödinger equations, two-grid methods, mixed finite element methods, coupled systems

**1. Introduction**

In physics, especially quantum mechanics, the Schrödinger equation is an equation that describes how the quantum state of a physical system changes in time [2, 5]. A nonlinear Schrödinger equation is a classical field equation with applications to optics and water waves. One general class of such equations takes the form

$$i\frac{\partial u}{\partial t} + \nabla \cdot (K\nabla u) = f(\mathbf{x}, u, \bar{u}, t), \quad (1)$$

where  $u = u_R + iu_I = (u_R, u_I)$  is the unknown complex valued function,  $\mathbf{x}$  is the space variable,  $\bar{u}$  is the complex conjugate of  $u$ , and  $f$  is a nonlinear function of  $u$  and  $\bar{u}$ .

$K = \frac{r^2}{2m}$ , where  $r$  is the reduced Planck's constant, often very small, and  $m$  is the mass of the particle.

It is Xu who first demonstrates the two-grid approach (see [10, 11]) to the use of coarse and fine grids with a Galerkin finite-element method to solve nonlinear problems efficiently. In [6], Xu and his collaborators propose two-grid discretization techniques to decouple partial differential equations, e.g., the steady state Schrödinger-type equation. Dawson and Wheeler [3] apply the two-grid idea to mixed finite-element discretizations in which, for a single real-valued reaction diffusion equation,

$$\frac{\partial p}{\partial t} - \nabla \cdot (K \nabla p) = f(x, p), \quad (2)$$

the coefficient  $K$  depends upon the unknown but  $f$  does not. Wu and Allen [8] extend the mixed method and the two grid method to handle the nonlinear reaction term  $f(p)$ .

To be more specific, equation (2) has an equivalent first-order system:

$$\begin{aligned} \frac{\partial p}{\partial t} + \nabla \cdot \mathbf{v} &= f(x, p) && \text{mass balance,} \\ K^{-1} \mathbf{v} + \nabla p &= 0 && \text{flux law,} \end{aligned} \quad (3)$$

where  $\mathbf{v} = -(K \nabla p)$  is the diffusive flux. In many applications it is important to solve for  $p$  and  $\mathbf{v}$  with comparable accuracy (see [4]), also one must accommodate the nonlinear reaction term  $f(x, p)$  by linearizing and using an efficient iterative scheme.

In this paper, we examine two-grid mixed finite element methods for solving unsteady state Schrödinger equations of the form (1) with nonlinear reaction terms. The main emphases of our methods are twofold: first, to obtain accurate discrete approximations for both the concentrations and their fluxes and, second, to implement efficient iterative schemes for solving the nonlinear discretized equations.

Let  $\phi(\mathbf{x})$  be a complex valued function. We denote  $\phi_R(\mathbf{x})$  and  $\phi_I(\mathbf{x})$  as its real part and imaginary part, respectively. Then  $\phi(\mathbf{x}) = \phi_R(\mathbf{x}) + i\phi_I(\mathbf{x})$  can be represented as a vector function  $(\phi_R(\mathbf{x}), \phi_I(\mathbf{x}))$ . In the remainder of the paper, Section 2 reviews the two-grid method and associated numerical schemes, analyzed in detail in the earlier paper [8]. In Section 3, we apply the two-grid approach to time dependent nonlinear Schrödinger equations, then in the next Section 4, numerical experiments are provided to the efficiencies of the orchestrations. Section 5 draws conclusions.

## 2. Review of the Two-Grid Approach

In this section, we review a two-grid method to solve the single reaction-diffusion equation (2) on a rectangular domain  $\Omega \in R^2$ . Here,  $p$  is the unknown potential,  $K$  is a positive function of space,  $\mathbf{v} = -K\nabla p$  is the flux, and  $f$  is the nonlinear reaction term. This review serves as a foundation for the extension to reaction-diffusion systems, the Schrödinger type equations.

### 2.1. Mixed Finite-Element Discretization

We start with a brief review of the mixed finite-element discretization for equation (2). On the rectangular domain  $\Omega = [0, 1] \times [0, 1]$ , let  $\Delta^x = \{0 = x_0 < x_1 < \dots < x_m = 1\}$  be a grid on  $x$ -axis, and let  $\Delta^y = \{0 = y_0 < y_1 < \dots < y_n = 1\}$  be a grid on  $y$ -axis. Then  $\Delta^x \times \Delta^y$  is a rectangular grid on  $\Omega$ , having nodes  $(x_i, y_j)$ . For convenience, we use grids having uniform mesh size  $h$ , but it is possible to relax this condition. Later, in the two-grid linearization, we use  $h$  to denote the mesh size of the fine grid, which we denote as  $\Delta_h$ .

Based on this grid, we use standard, lowest-order Raviart-Thomas trial spaces  $W_h$  and  $Q_h$  to approximate  $p$  and  $\mathbf{v}$ , respectively, see [7]. Let

$$l_i(x) = \begin{cases} \frac{x-x_{i-1}}{h}, & \text{for } x_{i-1} < x \leq x_i \\ \frac{x_{i+1}-x}{h}, & \text{for } x_i < x \leq x_{i+1} \end{cases} \quad c_i(x) = \begin{cases} 1, & \text{for } x_{i-1} < x \leq x_i \\ 0, & \text{for otherwise} \end{cases}$$

The potential space  $W_h = \text{span}\{c_i(x)c_j(y)\}$  consists of functions that are piecewise constant on  $\Delta_h$ . The flux space is  $Q_h = Q_h^x \times Q_h^y$ , where  $Q_h^x = \text{span}\{l_i(x)c_j(y)\}$  contains functions that are piecewise linear and continuous on  $\Delta^x$  and piecewise constant on  $\Delta^y$ , while  $Q_h^y = \text{span}\{c_i(x)l_j(y)\}$  contains functions that are piecewise constant on  $\Delta^x$  and piecewise linear and continuous on  $\Delta^y$ .

Equation (2) is equivalent to the first order system (3). Discretizing implicitly in time via the approximation  $\left(\frac{\partial p_h}{\partial t}\right)^n \simeq \frac{1}{\Delta t}(p_h^n - p_h^{n-1})$ , the mixed finite-element approximation to this system is as follows: At the  $n$ -th time step ( $t = n\Delta t$ ), find an approximate potential  $p_h^n \in W_h$  and an approximate flux  $\mathbf{v}_h^n \in Q_h$  such that

$$\begin{aligned} \int_{\Omega} K^{-1} \mathbf{v}_h^n \cdot \mathbf{q}_h - \int_{\Omega} p_h^n \nabla \cdot \mathbf{q}_h &= 0, & \text{for all } \mathbf{q}_h \in Q_h, \\ \int_{\Omega} w_h \nabla \cdot \mathbf{v}_h^n + \int_{\Omega} w_h \frac{1}{\Delta t} (p_h^n - p_h^{n-1}) &= \int_{\Omega} w_h f(p_h^n), & \text{for all } w_h \in W_h. \end{aligned} \tag{4}$$

### 2.2. Linearization via the Two-Grid Approach

To solve the mixed-method system, we use a two-grid scheme, which relegates the computational effort of nonlinear iterations to a coarse subgrid  $\Delta_H \subset \Delta_h$ , having mesh size  $H \gg h$ . Associated with  $\Delta_H$  are trial spaces  $Q_H$  and  $W_H$  analogous to  $Q_h$  and  $W_h$  on fine grid  $\Delta_h$ . We compute the trial functions  $p_H^n \in W_H$  and  $\mathbf{v}_H^n \in Q_H$  using an iterative Newton-like approximation, described shortly, to the mixed-method equations on  $\Delta_H$ . Once we have computed  $p_H^n$  and  $\mathbf{v}_H^n$ , we use them to initialize a single iteration for the unknowns  $p_h^n$  and  $\mathbf{v}_h^n$  associated with the fine grid. We now review this scheme.

To obtain the coarse-grid iterative scheme, we adopt the first order Taylor expansion: At time level  $n$ , the  $m$ -th iterate,  $f(p_H^{n,m})$  can be replaced by

$$f(p_H^{n,m}) \simeq f(p_H^{n,m-1}) + f'(p_H^{n,m-1})(p_H^{n,m} - p_H^{n,m-1}). \tag{5}$$

Substituting this expression into the weak form (4) and rearranging, on the coarse grid, we solve the following equations iteratively.

$$\int_{\Omega} K^{-1} \mathbf{v}_H^{n,m} \cdot \mathbf{q}_H - \int_{\Omega} p_H^{n,m} \nabla \cdot \mathbf{q}_H = 0, \quad \text{for all } \mathbf{q}_H \in Q_H,$$

$$\int_{\Omega} w_H \nabla \cdot v_H^{n,m} + \int_{\Omega} w_H \left[ \frac{1}{\Delta t} - f'(p_H^{n,m-1}) \right] p_H^{n,m}$$

$$= \int_{\Omega} w_H \left[ \frac{1}{\Delta t} p_H^{n-1} + f(p_H^{n,m-1}) - f'(p_H^{n,m-1}) p_H^{n,m-1} \right], \quad \text{for all } w_H \in W_H.$$

Next, to obtain the fine-grid approximations  $p_h^n$  and  $\mathbf{v}_h^n$ , we interpolate  $p_H^n$  to  $\Delta_h$  and adopt the Taylor expansion

$$f(p_h^n) \simeq f(p_H^n) + f'(p_H^n)(p_h^n - p_H^n). \tag{6}$$

Substituting this expansion into the weak form (4), on the fine grid, we solve the following linear system once:

$$\int_{\Omega} K^{-1} \mathbf{v}_h^n \cdot \mathbf{q}_h - \int_{\Omega} p_h^n \nabla \cdot \mathbf{q}_h = 0, \quad \text{for all } \mathbf{q}_h \in Q_h,$$

$$\int_{\Omega} w_h \nabla \cdot \mathbf{v}_h^n + \int_{\Omega} w_h \left( \frac{1}{\Delta t} - f'(p_H^n) \right) p_h^n$$

$$= \int_{\Omega} w_h \left( \frac{1}{\Delta t} p_h^{n-1} + f(p_H^n) - f'(p_H^n) p_H^n \right), \quad \text{for all } w_h \in W_h. \quad (7)$$

This linearization is efficient only when the coarse grid  $\Delta_H$  is much coarser than the fine grid  $\Delta_h$  without sacrificing the accuracy associated with the fine grid solution  $(p_h^n, \mathbf{v}_h^n)$ . Under reasonable hypotheses [8], in  $L^2$  norm, at  $t = N\Delta t$ , the fine-grid solution obeys error estimates of the form

$$\|p_h^N - p^N\| + \left[ \sum_{n=1}^N \Delta t \|K^{1/2}(\nabla p_h^n - \nabla p^n)\|^2 \right]^{1/2} \leq C \left( h^{k+1} + H^{2k+2} + \Delta t \right). \quad (8)$$

Here,  $k$  is related to the degree of polynomials used in the trial spaces  $W_H, W_h, Q_H$ , and  $Q_h$ . In particular, for the lowest-order Raviart-Thomas spaces used here,  $k = 0$ . Hence the  $L^2$  errors in the fine grid potential and flux are  $O(h + H^2 + \Delta t)$ . For proof and numerical corroboration, we refer to our previous paper [8].

### 3. Time-Dependent Nonlinear Schrödinger Equations

There are many nonlinear Schrödinger equations of which are perturbations [2] of the free Schrödinger equation, where  $f = 0$  in (1). In this section, we apply the two-grid approach to derive mixed finite element solution for this type of equations.

The complex valued equation (1) has its equivalent form as the coupled equations:

$$\begin{aligned} \frac{\partial u_R}{\partial t} + \nabla \cdot (K \nabla u_I) &= f_I(\mathbf{x}, u, \bar{u}, t), \\ \frac{\partial u_I}{\partial t} - \nabla \cdot (K \nabla u_R) &= -f_R(\mathbf{x}, u, \bar{u}, t). \end{aligned} \quad (9)$$

Introducing two flux variables as in the previous section, (9) can be written as two first order coupled systems as

$$\begin{aligned} s_I + K \nabla u_I &= 0, \\ \frac{\partial u_R}{\partial t} - \nabla \cdot (s_I) &= f_I(\mathbf{x}, u, \bar{u}, t), \\ s_R + K \nabla u_R &= 0, \\ \frac{\partial u_I}{\partial t} + \nabla \cdot (s_R) &= -f_R(\mathbf{x}, u, \bar{u}, t). \end{aligned} \quad (10)$$

### 3.1. The Two-Grid Approach

For the time-dependent problem, we discretize the time  $[0, T]$  as  $t_n = n\Delta t$ , where  $\Delta t = T/N$ ,  $N$  is the total number of time steps to take. Then at each time level, we apply the two-grid approach to solve the coupled nonlinear problems (10). To be consistent with our approach described earlier, in (10) we group the second and third equations, then the first and the last equations together.

Overall, at  $n$ -th time level, we seek solutions  $(u_{R_h}^n, s_{R_h}^n), (u_{I_h}^n, s_{I_h}^n) \in W_h \times Q_h$  by following (1) finding nonlinear approximations  $(u_{R_H}^n, s_{R_H}^n), (u_{I_H}^n, s_{I_H}^n)$  on the coarse grid  $W_H \times Q_H$ , then (2) performing a linear procedure to upgrade them on the fine grid.

In details, on the coarse grid, the  $m$ -th iteration,

*Step 1.* Compute  $u_{R_H}^{(n,m)}$  and  $s_{R_H}^{(n,m)}$  by solving

$$\int_{\Omega} s_{R_H}^{(n,m)} q_H - \int_{\Omega} u_{R_H}^{(n,m)} \nabla \cdot q_H = 0, \quad \text{for all } q_H \in Q_H,$$

$$\begin{aligned} & \int_{\Omega} -K \nabla \cdot s_{I_H}^{(n,m-1)} w_H \\ & + \int_{\Omega} \left( \frac{u_{R_H}^{(n,m)} - u_{R_H}^{n-1}}{\Delta t} - \frac{\partial f_I}{\partial u_R}(u_{R_H}^{(n,m-1)}, u_{I_H}^{(n,m-1)}) u_{R_H}^{(n,m)} \right) w_H \\ & = \int_{\Omega} \left( f_I(u_{R_H}^{(n,m-1)}, u_{I_H}^{(n,m-1)}) - \frac{\partial f_I}{\partial u_R}(u_{R_H}^{(n,m-1)}, u_{I_H}^{(n,m-1)}) u_{R_H}^{(n,m-1)} \right) w_H, \end{aligned}$$

for all  $w_H \in W_H$ . (11)

For brevity let us denote this procedure as for  $u_{R_H}^{(n,m)}, s_{R_H}^{(n,m)}$ ,

$$\mathcal{H}(u_{R_H}^{(n,m)}, s_{R_H}^{(n,m)}) = f_I(u_{R_H}^{(n,m)}, u_{I_H}^{(n,m-1)}).$$

*Step 2.* Similar to Step 1, we solve  $\mathcal{H}(u_{I_H}^{(n,m)}, s_{I_H}^{(n,m)}) = -f_R(u_{R_H}^{(n,m)}, u_{I_H}^{(n,m)})$  for  $u_{I_H}^{(n,m)}, s_{I_H}^{(n,m)}$ .

*Step 3.* Test convergence. If necessary, go for more iterations; otherwise, set  $u_{R_H}^n = u_{R_H}^{(n,m)}, s_{R_H}^n = s_{R_H}^{(n,m)}$ , and  $u_{I_H}^n = u_{I_H}^{(n,m)}, s_{I_H}^n = s_{I_H}^{(n,m)}$ , then move on to the fine grid.

On the fine grid, we interpolate  $u_{R_H}^n$  and  $u_{I_H}^n$  to the fine grid  $\Delta_h$ , and adopt the first order Taylor expansion

$$f_R(u_{R_h}^n, u_{I_H}^n) \simeq f_R(u_{R_H}^n, u_{I_H}^n) + \frac{\partial f_R}{\partial u_R}(u_{R_H}^n, u_{I_H}^n)(u_{R_h}^n - u_{R_H}^n). \tag{12}$$

For all  $w_h \in W_h$  and all  $q_h \in Q_h$ , we seek  $u_{R_h}^n$  and  $s_{R_h}^n$  by solving the following system

$$\begin{aligned} \int_{\Omega} s_{R_h}^n q_h - \int_{\Omega} K u_{R_h}^n \nabla \cdot q_h &= 0, \\ \int_{\Omega} -\nabla \cdot s_{I_H}^n w_h + \int_{\Omega} \left( \frac{u_{R_h}^n - u_{R_h}^{n-1}}{\Delta t} - \frac{\partial f_I}{\partial u_R}(u_{R_H}^n, u_{I_H}^n) u_{R_h}^n \right) w_h & \\ = \int_{\Omega} \left( f_I(u_{R_H}^n, u_{I_H}^n) - \frac{\partial f_I}{\partial u_R}(u_{R_H}^n, u_{I_H}^n) u_{R_H}^n \right) w_h. & \end{aligned} \tag{13}$$

Then by

$$f_I(u_{R_h}^n, u_{I_h}^n) \simeq f_I(u_{R_h}^n, u_{I_H}^n) + \frac{\partial f_I}{\partial u_I}(u_{R_h}^n, u_{I_H}^n)(u_{I_h}^n - u_{I_H}^n), \tag{14}$$

we solve for  $u_{I_h}^n$  and  $s_{I_h}^n$  from the system

$$\begin{aligned} \int_{\Omega} s_{I_h}^n q_h - \int_{\Omega} K u_{I_h}^n \nabla \cdot q_h &= 0, \\ \int_{\Omega} \nabla \cdot s_{R_h}^n w_h + \int_{\Omega} \left( \frac{u_{I_h}^n - u_{I_h}^{n-1}}{\Delta t} + \frac{\partial f_R}{\partial u_I}(u_{R_h}^n, u_{I_H}^n) u_{I_h}^n \right) w_h & \\ = \int_{\Omega} \left( -f_R(u_{R_h}^n, u_{I_H}^n) + \frac{\partial f_R}{\partial u_I}(u_{R_h}^n, u_{I_H}^n) u_{I_H}^n \right) w_h. & \end{aligned} \tag{15}$$

Both systems (13) and (15) are linear systems, we solve them once on the fine grid.

### 3.2. Matrix Structure and Numerical Linear Algebra

On both the coarse and fine grids, one must solve linear systems of the form

$$\begin{bmatrix} A & N \\ & M \end{bmatrix} \begin{bmatrix} S \\ U \end{bmatrix} = \begin{bmatrix} F_1 \\ F_2 \end{bmatrix}. \tag{16}$$

$S$  consists of two components as  $S = (S^x, S^y)^T$ , where  $S^x$  is the  $x$ -component of the flux,  $S^y$  is the  $y$ -component of the flux. Correspondingly,  $A = \begin{bmatrix} A^x & \\ & A^y \end{bmatrix}$ ,

$N = \begin{bmatrix} N^x \\ N^y \end{bmatrix}$ . Entries of  $A^x$  have the form  $\int_{\Omega} l_i(x)c_j(y)l_k(x)c_l(y)$ , entries of  $A^y$  have the form of  $\int_{\Omega} l_i(y)c_j(x)l_k(y)c_l(x)$ . By the product  $l_i l_k = 0$  when  $|i - k| > 1$ , and  $c_j c_l = 0$  when  $j \neq l$ , both  $A^x$  and  $A^y$  are tridiagonal and symmetric. Both  $N^x$  and  $N^y$  are sparse matrices. Entries of  $N^x$  are integrals of  $\int_{\Omega} l_i(x)c_j(y)l'_k(x)c_l(y)$ , entries of  $N^y$  are integrals of  $\int_{\Omega} l_i(y)c_j(x)l'_k(y)c_l(x)$ . Both forms vanish when  $k \neq i, i + 1$  or  $l \neq i$ .  $M$  is a diagonal matrix, positive definite and bounded away from zero. On the coarse grid,  $M$  contains diagonal entries of  $\left(\frac{1}{\Delta t} - \frac{\partial f_L}{\partial u_R}(u_{RH}^{(n,m-1)}, u_{IH}^{(n,m-1)})\right)$  as in Step 1, and  $\left(\frac{1}{\Delta t} + \frac{\partial f_R}{\partial u_I}(u_{RH}^{(n,m)}, u_{IH}^{(n,m-1)})\right)$  in Step 2. On the fine grid, diagonal entries of  $M$  have the form  $\left(\frac{1}{\Delta t} - \frac{\partial f_L}{\partial u_R}(u_{RH}^n, u_{IH}^n)\right)$  as in (13), and  $\left(\frac{1}{\Delta t} + \frac{\partial f_R}{\partial u_I}(u_{Rh}^n, u_{Ih}^n)\right)$  as in (15).

When  $\Delta t$  is relatively small, one can easily solve  $U = M^{-1}F_2$  first, then solve  $S$  as  $AS = F_1 - NU$ .

### 4. Numerical Experiments

In this section we provide some numerical results to demonstrate the efficiency of the two-grid mixed method for time-dependent Schrödinger type equations.

**Example.** Consider the following initial boundary value Schrödinger equation,

$$\begin{aligned} i \frac{\partial u}{\partial t} + \nabla \cdot (K \nabla u) &= |u|^2 u + f(\mathbf{x}, t), & \mathbf{x} \in \Omega, \\ u(\mathbf{x}, t) &= 0, & \mathbf{x} \in \partial\Omega, \end{aligned} \tag{17}$$

where  $\Omega = [0, 1]^2$ . The source function  $f(\mathbf{x}, t)$  is chosen such that the exact solution is  $u(\mathbf{x}, t) = (2+i)e^t \sin(\pi x) \sin(\pi y)$ , with flux variables  $s_R(\mathbf{x}, t) = -K \nabla u_R$ ,  $s_I(\mathbf{x}, t) = -K \nabla u_I$ . We again use the lowest Raviart-Thomas rectangular mixed finite element spaces with index  $k = 0$ . In all of the computations, we use  $K = 0.01$ ,  $\Delta t = 0.001$ , and examine the numerical results at  $t = 5\Delta t$ .

Table 1 shows how the  $L^2$  errors in  $u_h$ ,  $s_{R_h}$  and  $s_{I_h}$  shrink with  $h$  when  $H = h^{1/2}$ . Errors for  $u_h$  decrease linearly as  $h \rightarrow 0$ , even though the nonlinear iterations occur on a grid much coarser than  $h$ . Errors for  $s_{R_h}$  and  $s_{I_h}$  shrink near linearly.

The two grid strategy is efficient as it put nonlinear iterations on much coarse grid, and on the fine grid, only one linear system is needed. As shown in Figure 1,  $U_R$  is first computed on the coarse grid (left)  $H = 2^{-3}$ , then we only need to solve a linear problem on the fine grid (right)  $h = 2^{-6}$ . In Figure



$H$	$h$	$\ u_h - u\ $	$\ s_{R_h} - s_R\ $	$\ s_{I_h} - s_I\ $
$2^{-1}$	$2^{-2}$	$3.5494 \times 10^{-1}$	$1.0287 \times 10^{-2}$	$5.1473 \times 10^{-3}$
$2^{-2}$	$2^{-4}$	$8.9807 \times 10^{-2}$	$2.5228 \times 10^{-3}$	$1.2619 \times 10^{-3}$
$2^{-3}$	$2^{-6}$	$2.2417 \times 10^{-2}$	$6.3393 \times 10^{-4}$	$3.1528 \times 10^{-4}$
$2^{-4}$	$2^{-8}$	$5.6086 \times 10^{-3}$	$1.8912 \times 10^{-4}$	$1.7265 \times 10^{-4}$

Table 1: Decay of  $L^2$  errors with grid refinement, keeping  $H = h^{1/2}$

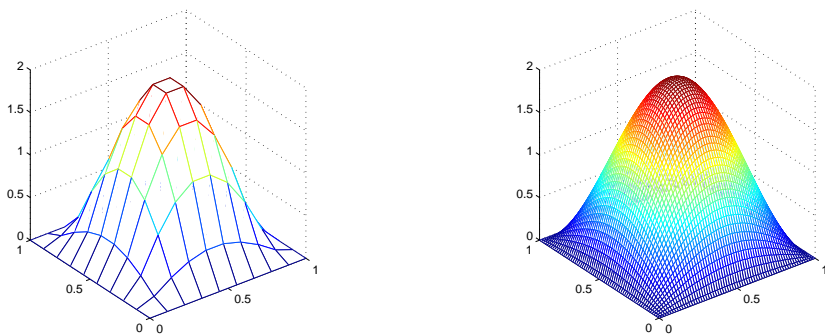


Figure 1: At  $t = 5\Delta t$ , (left) mesh plot for  $u_R$  on the coarse grid with  $H = 2^{-3}$  by Newton iterations; (right)  $u_R$  on fine grid with  $h = 2^{-6}$  by solving one linear system.

2, the left plot is for real valued flux  $S_R$  on the coarse grid  $H = 2^{-3}$ , the right plot is the fine grid  $h = 2^{-6}$  solution.

In Table 2, we fix the mesh size of fine grid as  $h = 2^{-8}$ , then vary with the mesh size  $H$  of the coarse-grid. Over the range of course grids tested, the fine-grid errors are quite insensitive to the coarseness of the grid on which we iterate. The table also shows estimates of total CPU times which give some indication of the efficiency of the two-grid approach. There is a significant range of coarse-grid mesh sizes over which the runtime efficiency and accuracy of the method are fairly insensitive. But choosing too fine a coarse grid sacrifices efficiency without improving accuracy. By far the longest runtime occurs when we use no coarse-grid iterations, that is, when  $H = h$ .

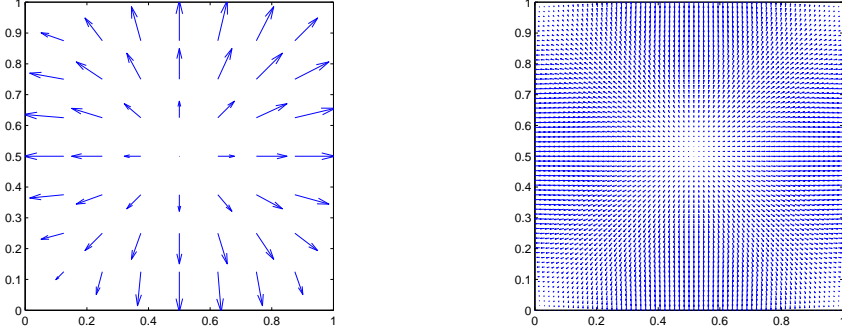


Figure 2: At  $t = 5\Delta t$ , (left) gradient field  $s_R(\mathbf{x}, t) = -K\nabla u_R$  on the coarse grid with  $H = 2^{-3}$  by Newton iterations; (right)  $s_R(\mathbf{x}, t)$  on fine grid with  $h = 2^{-6}$ .

$H$	$\ u_h - u\ $	time(s)	$H$	$\ u_h - u\ $	time(s)
$2^{-1}$	$5.63413 \times 10^{-3}$	26.360	$2^{-5}$	$5.60846 \times 10^{-3}$	27.406
$2^{-2}$	$5.61176 \times 10^{-3}$	26.375	$2^{-6}$	$5.60843 \times 10^{-3}$	30.484
$2^{-3}$	$5.60926 \times 10^{-3}$	26.438	$2^{-7}$	$5.60842 \times 10^{-3}$	45.359
$2^{-4}$	$5.60864 \times 10^{-3}$	26.656	$2^{-8}$	$5.62095 \times 10^{-3}$	63.047

Table 2:  $L^2$  errors for  $h = 2^{-8}$  versus coarse mesh size  $H$

## 5. Conclusions

The results reported here have shown that two-grid mixed finite-element methods are efficient on decoupling and solving nonlinear Schrödinger type equations. The methods preserve the  $\mathcal{O}(h)$  error estimates associated with the mixed finite-element discretization, provided the coarse-grid mesh size  $H$  satisfies  $H = \mathcal{O}(h^{1/2})$ . They yield significant speedups over single-grid methods, owing to their ability to concentrate most of the nonlinear iterations on coarse grids. We believe that the analysis would involve relatively straightforward translation of earlier results [8] to this new setting. The scheme produces a computationally attractive way to generate numerical solutions to other types of coupled differential equation systems. We hope to extend this method to the study of equations in different fields.

## References

- [1] M.B. Allen, R.E. Ewing, P. Lu, Well conditioned iterative schemes for mixed finite-element models of porous-media flows, *SIAM Jour. Sci. Stat. Comput.*, **13**, No. 3 (1992), 794-814.
- [2] I. Bialynicki-Birula, M. Cieplak, Kaminski, *Theory of Quanta*, Oxford University Press Inc. (1992).
- [3] C.N. Dawson, M.F. Wheeler, Two-grid methods for mixed finite element approximations of nonlinear parabolic equations, *Contemp. Math.*, **180** (1994), 191-203.
- [4] J. Douglas, R. Ewing, M. Wheeler, The approximation of the pressure by a mixed method in the simulation of miscible displacement, *RAIRO Analyse Numérique*, **17**, No. 1 (1983), 17-33.
- [5] K. Hannabuss, *An Introduction to Quantum Theory*, Oxford University Press Inc. (1997).
- [6] J. Jin, S. Shu, J. Xu, A two-grid discretization method for decoupling systems of partial differential equations, *Mathematics of Computation*, **75**, No. 256 (2006), 1617-1626.
- [7] P.A. Raviart, J.M. Thomas, A mixed finite element method for second order elliptic problems, In: *Mathematical Aspects of the Finite Element Method* (Ed-s: I. Galligani, E. Magenes), Lecture Notes in Mathematics, **606**, Springer-Verlag, New York (1977).
- [8] Li Wu, M.B. Allen, A two-grid method for mixed finite-element solution of reaction-diffusion equations, *Numer. Meth. PDE*, **15** (1999), 317-332.
- [9] Li Wu, M.B. Allen, Two-grid methods for mixed finite-element solutions of coupled reaction-diffusion systems, *Numer. Meth. PDE*, **15** (1999), 589-604.
- [10] J. Xu, A novel two-grid method for semilinear equations, *SIAM J. Sci. Comput.*, **15**, No. 1 (1994), 231-237.
- [11] J. Xu, Two grid finite element discretization techniques for linear and nonlinear PDE, *SIAM Jour. Numer. Anal.*, **33**, No. 5 (1996), 1759-1777.

476